Competition between intra-community and inter-community synchronization and relevance in brain cortical networks

Ming Zhao,[1,2,3,*] Changsong Zhou,[4,†] Jinhu Lü,[5,‡] and Choy Heng Lai[1,2,§]

[1]*Department of Physics, National University of Singapore, Singapore 117542*

[2]*Beijing-Hong Kong-Singapore Joint Center of Nonlinear and Complex Systems (Singapore), Singapore 117542*

[3]*College of Physics and Technology, Guangxi Normal University, Guilin 541004, P. R. China*

[4]*Department of Physics, Centre for Nonlinear Studies, and Beijing-Hong Kong-Singapore Joint Centre for Nonlinear and Complex Systems (Hong Kong), Hong Kong Baptist University, Kowloon Tong, Hong Kong, P. R. China*

[5]*Key Laboratory of Systems and Control, Institute of Systems Science, Academy of Mathematics and Systems Science, Chinese Academy of Science, Beijing 100080, P. R. China*

(Received 17 January 2011; revised manuscript received 25 May 2011; published 25 July 2011)

In this paper the effects of inter-community links on the synchronization performance of community networks, especially on the competition between individual community and the whole network, are studied in detail. The study is organized from two aspects: the number or portion of inter-community links and the connection strategy of inter-community links between different communities. A critical point is found in the competition of global network and individual communities. Increasing the number of inter-community links will enhance the global synchronizability but degrade the synchronization performance of individual community before this point. After that the individual community will synchronize better and better as part of the whole network because the community structure is not so prominent. The critical point represents a balance region where the individual community is maximally independent while the information transmission remains effective between different communities. Among various connection strategies, connecting nodes belonging to different communities randomly rather than connecting nodes with larger degrees are the most efficient way to enhance global synchronization of the network. However, the dynamical modularity is the reverse case. A preferential connection scheme linking most of the hubs from the communities will allow rather efficient global synchronization while maintaining strong dynamical clustering of the communities. Interestingly, the observations are found to be relevant in a realistic network of cat cortex. The synchronization state is just at the critical point, which shows a reasonable combination of segregated function in individual communities and coordination among them. Our work sheds light on principles underlying the emergence of modular architectures in real network systems and provides guidance for the manipulation of synchronization in community networks.

DOI: 10.1103/PhysRevE.84.016109 PACS number(s): 89.75.Fb, 05.45.Xt, 87.18.Sn

I. INTRODUCTION

Communities exist ubiquitously in all kinds of networks [1–3], and synchronization on community networks is of great importance in biological and social networks. To date, the synchronization property of community networks has been well studied. It has been shown that the sparsity of connections between different communities hinders the global synchronization of complex networks [4–6]. Factors that affect the synchronization of community networks have been intensively studied, and strategies that can achieve global synchronization have been proposed [7–10]. Synchronization transition process of community networks has also been studied [11,12]. Utilizing synchronization to detect community structure has attracted a great deal of attention recently [13–17]. Moreover, the dynamical modules of networks with and without clear communities have also been studied in detail [18–22]. Very recently, a class of small-world networks with spatial and network modularity were obtained by evolving the arrangement of nodes in space and their corresponding network topology [23]. Besides, some other interesting topics, such as the synchronization interfaces and overlapping communities in complex networks, were also studied [24].

Most of the previous studies on synchronization in community networks were based on various community network models rather than on real-world networks. Recently, in the context of the balance of functional segregation and integration in neural systems, we defined a complexity measure of the synchronization state of networks that enables both segregation and integration, and we found that heterogeneous degree distribution and community structure support high complexity [22]. More interestingly, we found that the cortical network of cats (which has four communities) has optimal complexity compared to various rewired networks. However, the dynamical mechanism underlying these observations is not known yet.

The analysis in the present work will elucidate this dynamical mechanism through a detailed study of the synchronization state of community networks from two levels: global network and individual community. Interestingly, we observe a phenomenon that has been ignored in the study of synchronization of modular network: competition between these two levels. This competition has great relevance to real-world community systems: functional segregation requires independency of individual communities from the others through coordination

*zhaom17@gmail.com
†cszhou@hkbu.edu.hk
‡jhlu@iss.ac.cn
§phylaich@nus.edu.sg

synchronization within community, but weak interference between communities (weak global synchronization), while integration requires strong enough coordinations between communities (strong global synchronization). We believe that there is an optimal balanced point for community networks, and the structure of real-world community systems could be close to such a critical point. In this paper, we identify the critical point by investigating the change of synchronization of community and global network as a function of modularity. We are pleased to find that the cat cortical network is at this critical point.

Another interesting problem that long has been neglected is that even at the same modularity the connection strategy of inter-community links (links connecting nodes belong to different communities) could greatly affect the synchronization property of community networks, which will be intensively studied in this paper. This work is organized as follows: In the next section, we introduce the dynamical equation of each node and the community network model. In Sec. III, we discuss the competition between the individual community and the whole network induced by the number of inter-community links. The effects of the connection strategy of the inter-community links on the competition will be discussed in Sec. IV. Then we study the synchronization competition of cat cortical network. We will give our discussion and conclusion in the last section.

II. DYNAMICAL EQUATION AND COMMUNITY NETWORK MODEL

To investigate the synchronization on complex networks, dynamical systems are often taken as nodes and the couplings between different systems are the links; thus the dynamical equation of each node in a complex network with N nodes is

$$\dot{\mathbf{x}}_i = \mathbf{F}(\mathbf{x}_i) - \frac{\sigma}{\langle k\rangle}\sum_{j=1}^{N} G_{ij}\mathbf{H}(\mathbf{x}_j), \quad i = 1,\ldots,N, \tag{1}$$

where $\dot{\mathbf{x}} = \mathbf{F}(\mathbf{x})$ is the individual dynamics, σ is the overall coupling strength, $\langle k\rangle$ is the average degree of undirected or average in-degree of directed network, $\mathbf{H}(\mathbf{x})$ is the output function, and G_{ij} is the element of coupling matrix. In our simulations, if node i is coupled by node j, $G_{ij} < 0$, otherwise $G_{ij} = 0$, and the diagonal element $G_{ii} = -\sum_{j=1,j\neq i}^{N} G_{ij}$ to ensure the sum of the elements in a row is 0 so as to make the synchronization manifold an invariant manifold. In much previous work, the global network synchronizability was measured by the eigenvalues of the coupling matrix without calculating the iteration of oscillators on the networks according to the master stability function [25,26]. In this paper, we study not only the global network synchronizability but also the individual community synchronization performance; thus the master stability function is insufficient to our study, so we take the Rössler oscillator as a dynamical node to fulfill our simulation:

$$\begin{aligned}\dot{x} &= -y - z,\\ \dot{y} &= x + ay,\\ \dot{z} &= b + z(x - c),\end{aligned} \tag{2}$$

where $a = 0.2$, $b = 0.2$, and $c = 7.0$. We take the output function $\mathbf{H}(\mathbf{x}) = (x,0,0)$. In Secs. II and III, all the links are unweighted and the coupling matrix is Laplacian matrix; i.e., $G_{ij} = -1$ (node i and j are connected) or $G_{ij} = 0$ (node i and j are not connected) for off-diagonal elements, and $G_{ii} = k_i$ for diagonal elements. The correlation between each pair of nodes c_{ij} is calculated to measure the synchronization performance, and the average correlations of all pairs of nodes in the whole network C_N and that of pairs in a community C_C are taken as the measure of the synchronization performance of the global network and individual community, respectively.

To implement our study effectively, we design the following community network model: Take m networks as subnetworks to generate a community network and these subnetworks will be the communities, then rewire the intra-community links (links connecting nodes within the same community) to inter-community links with various strategies, which will be discussed in detail. When more and more inter-community links emerge, the modularity will decrease gradually till the network becomes a homogeneous one.

We follow Refs. [27,28] to quantify modularity of a network with m communities as

$$Q = \sum_{l}^{m}\left(e_{ll} - a_l^2\right), \tag{3}$$

where $a_l = \sum_k^m e_{lk}$ and e_{lk} is the fraction of total strength of the links in the network that connect the nodes between the communities l and k, namely, $e_{lk} = (1/W)\sum_{i\in l, j\in k} w_{ij}$, with w_{ij} being the connection strength between two nodes and W the total of w_{ij} in the network. In previous studies it has been found that synchronization clusters emerge during the transition to synchronization in random and scale-free [19,29] networks, and in our work, we have found that this phenomenon can be very prominent when community structure in networks exists. The synchronization clusters may be very clear at some coupling strength and hard to find at other coupling strength values. To measure the strength of the synchronization cluster, we generalize the definition of modularity and define a dynamical modularity. To make sure the two modularities are not confused we name the modularity in Eq. (3) the topological modularity Q_T to measure the strength of community structure from the adjacency matrix of the network. We measure the strength of synchronization clustering by the dynamical modularity Q_D, which is computed by taking w_{ij} as the dynamical dependency between two nodes. In particular, $w_{ij} = |\bar{c}_{ij}|$, where $\bar{c}_{ij} = (c_{x,ij} + c_{y,ij} + c_{z,ij})/3.0$ is the average correlation over the three variables between a pair of nodes i and j. We get the correlation between nodes by integrating Eq. (1) using the Runge-Kutta method with step size $h = 0.05$; after a transient time interval $t_0 = 700$, we store the data till $T = 1200$ and calculate $c_{x,ij} = [\frac{1}{(T-t_0)/h}\sum_{t=t_0/h}^{T/h}(x_{i,t} - \bar{x}_i)(x_{j,t} - \bar{x}_j)]/(\sigma_{x_i}\sigma_{x_j})$, where $\bar{x}_i$ and σ_{x_i} are the average and standard deviation of variable x_i over the time interval from t_0 to T, and $c_{x,ij}$ takes values from -1 to 1. The dynamical modularity Q_D will be large, when the nodes between different dynamical clusters have weak or no correlation, and Q_D will decrease with the increasing of dependency between nodes belonging to different dynamical

clusters, no matter the dependency is in phase or antiphase according to the definition of w_{ij}.

III. COMPETITION CAUSED BY INTER-COMMUNITY LINK NUMBER

In this section, we construct community networks by four equal-sized Erdos-Renyi (ER) random networks [30,31], and each has 100 nodes with the average degree 16. We construct community networks with the following operations: (1) random select an intra-community link, (2) cut one end of it, and (3) rewire it to a random selected node in the other subnetworks. Only after several rewirings, the whole network will become connected. Repeat the operations 1–3 till the desired community network is obtained. This connection strategy is called *random connection*. When more and more intra-community links are changed to inter-community links, the topological modularity Q_T becomes smaller and smaller till the network becomes fully random without communities.

In Figs. 1(a) and 1(b), we present the changes of C_N and C_C with coupling strength σ at different topological modularity Q_T (corresponding to different number of inter-community links L_E). Clearly, at the same coupling strength, the global network synchronizability will be better and better with the decreasing of topological modularity Q_T, which is consistent with previous studies [4–6]. However, the change of global synchronization performance with respect to the coupling strength σ is greatly different from the monotonic dependence on Q_T: All the curves first increase sharply at very small coupling strength [region I in Fig. 1(a)] and then increase slowly in a broad region of coupling strength (region II). With the further increasing of σ, networks with fewer inter-community links (larger Q_T) will show degraded synchronization performance, while those with more inter-community links will be much better (region III). After that all the curves will reach a saturated state (region IV). The synchronization performance of individual community, C_C behaves in the opposite way. It increases monotonically with σ but does not show a monotonic dependence on the topological modularity Q_T, as seen in Fig. 1(b). We will investigate the change of C_C with respect to Q_T in more detail later in this paper. We also study the effects of inter-community links on dynamical modularity Q_D. Figure 1(c) shows that Q_D has a main maximal point in region III and some other smaller maxima in regions I and II. For a complex community network system, larger dynamical modularity would favor segregated function by the communities, and meanwhile the communication between different dynamical clusters should also be smooth enough to make good coordination among them. Then a natural question arises: What is the best topological modularity where segregated function and coordination among them could be both satisfied? In the following, we try to present an insightful understanding to this question.

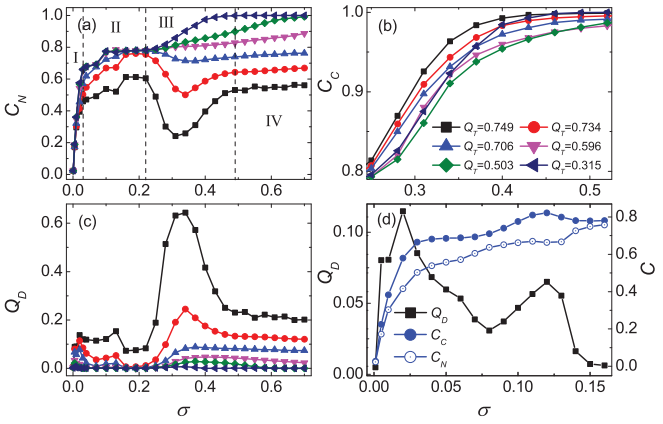

FIG. 1. (Color online) The synchronization performance of global network C_N (a), of individual community C_C (b), and dynamical modularity Q_D (c) as functions of the coupling strength σ at different topological modularity Q_T. (d) C_N, C_C, and Q_D at very small coupling strength for $Q_T = 0.734$. There are four communities in the network; each one is an ER random network with 100 nodes, and the average degree in each community is 16. Each plot is obtained after averaging over 50 network configurations and 10 initial states of each configuration.

First, we will investigate the mechanism of the phenomena in Fig. 1. As seen in Fig. 1(d) for the region of small couplings, C_C grows faster than C_N, leading to enhanced dynamical modularity. Then C_N becomes large too, and the dynamical clusters become smeared and Q_D is reduced. It worth mentioning that very small coupling strength could make the network go into a very good phase synchronization state, and at the coupling strength $\sigma = 0.030$ the initial isolated subnetworks will reach a complete synchronization state. To show explicitly the synchronization state of nodes in different communities, we plot the time series of the variable $x(t)$ of four typical nodes. We randomly pick out two communities from the four ones and select two nodes (not directly connected) in each community, one node having some inter-community links and the other one having only intra-community neighbors. By comparing the time series of the four nodes in Fig. 2(a), we found that phase synchronization throughout the networks occurs at very small coupling strength even for very few inter-community links. This corresponds to the slowly increasing region of C_N [region II in Fig. 1(a)]. With the further increase of the coupling strength, the networks move to a regime of fierce competition: For the networks with very few inter-community links, the individual community gets ready to reach complete synchronization state and the synchronization of nodes in the same community is rather good, but because of the random initial states, different communities oscillate at different phase, and the small number of inter-community links fail to bring the phases of different communities to each other; thus the global synchronization shows even worse performance compared to weaker coupling strength. This phenomenon can be seen in Fig. 2(b). The good synchronization performance within individual communities and weak synchronization between them result in the prominent dynamical modularity [region III, Figs. 1(a) and 1(c)]. As for the networks with enough inter-community links, communities yield to the effects of inter-community links, and there is no significant difference between intra-community synchronization and inter-community synchronization [Fig. 2(c)], leading to reduced dynamical modularity Q_D [Fig. 1(c)]. When the number of inter-community links is between these two situations, the individual community tries to oscillate as much independently as possible, but is inevitably affected by the others to some

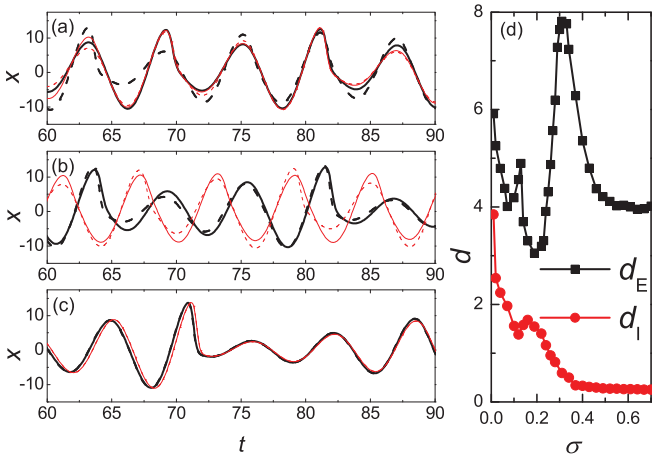

FIG. 2. (Color online) The change of state x with time t at coupling strength (a) 0.2, (b) 0.3, and (c) 0.6. The two bold curves and two regular curves present nodes belonging to the two different communities separately; the two solid curves represent nodes connected by inter-community link, and the two dashed curves present two nodes that are connected neither to each other nor to the other two nodes. (d) Change of d_E (square line) and d_I (circle line) with the coupling strength. The topological modularity of the adopted network is 0.746, and the other network parameters are the same as in Fig. 1.

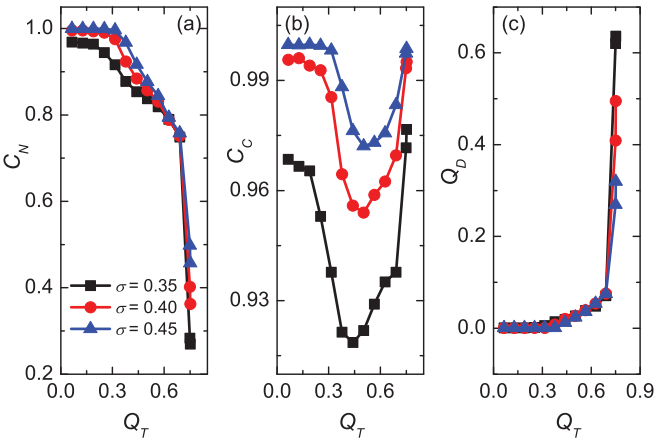

FIG. 3. (Color online) The change of C_N (a), C_C (b), and Q_D (c) with Q_T at various coupling strength σ as indicated. The other network parameters are the same as in Fig. 1.

extent, which results in degraded synchronization performance of individual communities. This is the reason for the decreasing of C_C at some topological modularity Q_T [Fig. 1(b)]. When the coupling strength becomes stronger and stronger, the information is exchanged more smoothly between different communities, and the states of different communities oscillate almost fully synchronously [Fig. 2(c)]. The global synchronization increases again, and the dynamical communities become not so prominent. This procedure of competition and coordination can be further manifested by the state differences of a node to its neighbors in the same community (d_I) and in the other communities (d_E). Here the difference for a node i and its neighbors in community X is defined as $d_i = \sqrt{\langle(\bar{x}_{j,X} - x_i)^2\rangle}$, where $\bar{x}_{j,X}$ is the average state of i's neighbors in community X and $\langle\cdot\rangle$ denotes averaging over time. d_I and d_E averaged over nodes are shown as functions of connection strength σ in Fig. 2(d). It is evident that d_I almost keeps decreasing with σ, which indicates that the state of a node gets close to its neighbors in the same community gradually. However, the curve of d_E has a distinct peak at about $\sigma^* = 0.3$, which shows that in this region of coupling strength the state of a node is far away from its neighbors in the other communities. In summary, we can see that at very weak coupling strength, the inter-community links could effectively transmit the state information of different communities to make the nodes of the whole network have the similar phase, and at very strong coupling strength, the inter-community links could also be efficient to bring together the states of different communities. However, when the coupling strength is between these two cases, the synchronization in communities are too strong, and the inter-community links fail to synchronize them at some larger topological modularity.

We also investigate C_N, C_C, and Q_D as functions of the topological modularity Q_T with fixed coupling strengths (Fig. 3). The inverse change between C_N and Q_D can be seen more obviously: The synchronization performance of global networks is degraded with the increasing of Q_T, and dynamical modularity Q_D will keep about zero at small Q_T and increase sharply when the community structure becomes prominent enough at large Q_T. Interesting behavior happens for synchronization of individual communities where C_C displays a pronounced minimum. The change of C_C can be understood as follows: When intra-community links are rewired to inter-community links in the beginning (Q_T decreasing), the number of intra-community links is reduced, and the number of inter-community links is increased, synchronization within community becomes weaker. In fact, only decreasing the number of intra-community links or only increasing the number of inter-community links will both reduce C_C. At this stage, the individual communities still oscillate largely independently ($C_C \sim 1 > C_N$). When there are enough inter-community links, as part of the whole network the individual communities are not prominent at all and no longer independent and $C_C \approx C_N$, corresponding to $Q_D \approx 0$. Therefore, the minimum of C_C corresponds to a critical point Q_{TC}. When $Q_T > Q_{TC}$, communities oscillate rather independently, and the communication between communities is weak, and for $Q_T < Q_{TC}$, the communication between communities is smooth but the dynamical independency of individual community is not prominent. Therefore, the region around the critical point represents a balance region where the individual community is still clearly independent while the information transmission remains effective between different communities.

It is worth noting that the best topological modularity Q_{TC} is relevant to the individual node dynamics, and the value may be of great difference for different types of node dynamics.

IV. COMPETITION UNDER VARIOUS CONNECTION STRATEGIES

Intuitively, not only the number of inter-community links but also the connection strategy of inter-community links

could affect the synchronization performance of community networks. For example, connecting nodes from different communities with larger degrees seems to be more efficient for information exchange between the communities and, therefore, might be superior for global synchronization. It has been found that in brain networks there are hub nodes (nodes with rather large degree), and some of them act as connectors between different communities [32,33]. In this section we design several connection strategies to investigate whether it will be better for global network synchronization to connect nodes with larger degree rather than nodes with smaller degree and how the competition will change with different connection strategies.

In this section we need the subnetworks with broader distribution of degree, and the Barabasi-Albert (BA) scale-free network model [34] seems a good candidate for our study, since its degree distribution obeys a power law, which allows the existence of nodes with rather larger degree than the average degree. Although there will be small synchronization clusters in communities during the synchronization process, we pay more attention to overall synchronization of individual community and the global network. The result will not be affected greatly by the synchronization clusters with small sizes.

The connection strategies are as follows: Take BA scale-free networks as communities and (1) keep one end of inter-community links on some nodes with largest degree (big nodes) and connect the nodes with randomly selected nodes in other communities (*hub-random connection*), (2) connect nodes selected in different communities with probability $p \propto k_i^{\alpha}$, where k_i is the degree of node belongs to the community and α is a tunable parameter (*preferential connection*), and (3) connect big nodes belong to different communities (*hub-hub connection*). Compared to the random connection, these three connection strategies make the distribution of inter-community links biased more and more to some big nodes. For preferential connection, with the increasing of parameter α, more and more inter-community links will connect nodes with larger degree. Suitably selected α will make the big nodes of different communities not only connect densely among themselves, but also connect to some *smaller* nodes. Such a connection scheme is consistent with the structure of brain cortex network that the hub areas are almost fully connected among themselves to form a hypercommunity overlapping different communities [35]. Moreover, to compare the effects of degree of connected nodes, we also designed the *middle* or *small degree connection* strategy, which is characterized by connecting nodes with middle or small degree in different communities. For all the strategies, once the inter-community link number is fixed, the topological modularity is almost the same according to the definition of modularity. Now we will see if the synchronization property will be different for the same topological modularity but different connection strategies.

We have investigated networks composed by different number of communities and found no essential differences in the synchronization property. Thus, in our simulation of this section we take the simplest community network model with two communities. Figure 4 shows the change of C_N, C_C, and Q_D with the coupling strength for community

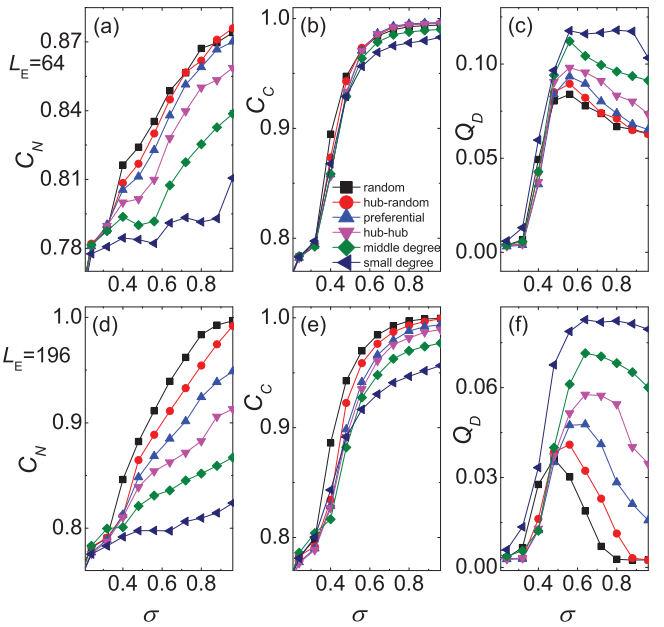

FIG. 4. (Color online) The change of C_C, C_N, and Q_D with σ at $L_E = 64$ ($Q_T = 0.46$) and 196 ($Q_T = 0.38$) for different rewiring strategies. Parameter $\alpha = 4.0$ for preferential connection. There are two communities in the network, each one is a BA network with 100 nodes, and the average degree is 16. Each plot is obtained after the averaging of 50 network configurations and 10 initial states of each configuration.

networks with different connection strategies. In contrast to intuitive expectation, not the strategy connecting only big nodes but that connecting random selected nodes will make the global network as well as individual community synchronization better at the same coupling strength and the same topological modularity. Namely, when the inter-community links distribute more homogeneously on nodes with different degree, the global network synchronization will be better. When the inter-community links concentrate on nodes with either large or small degrees, connecting big nodes will ensure better global network synchronization. As to the dynamical modularity, its values still changes inverse to the global network synchronizability. Q_D keeps larger in a broad range of coupling strength σ when the inter-community links are more concentrated to nodes with smaller degrees.

Now it is interesting to investigate how the connection strategy affects the competition between the synchronization of individual community and the whole network. In Fig. 5, we present the change of C_N, C_C, and Q_D with the topological modularity at several coupling strengths for community networks constructed by random connection, hub-random connection, preferential connection with parameter $\alpha = 2.0$ and 4.0, and hub-hub connection. From the figure it can be seen that when the inter-community links are more and more concentrated on hub nodes, the global network synchronization becomes too weak, and accordingly, the dynamical modularity is more prominent. The connection strategies have significant impact on the competition between individual community and global network. The critical point of topological modularity Q_T corresponding to the minimum of Q_C becomes smaller and smaller and finally disappears

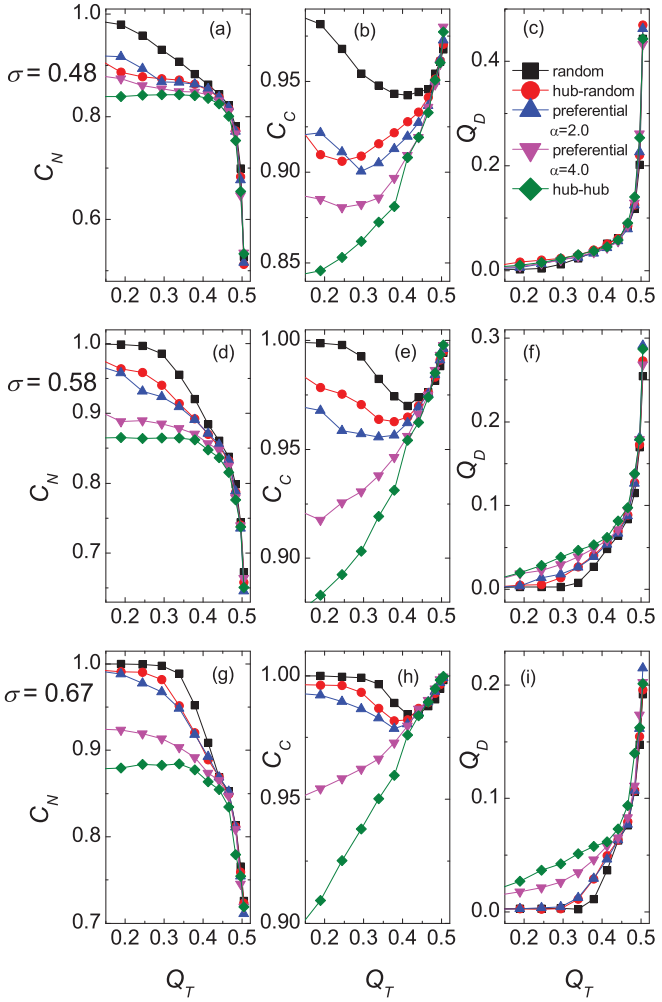

FIG. 5. (Color online) The change of C_C, C_N, and Q_D with σ for different rewiring strategies. The other network parameters are the same as in Fig. 4.

when the inter-community links are concentrated on hub nodes. The absence of the critical point shows the individual community dose not yield to each other. As a result, the coordination among communities is rather inefficient when the inter-community links too much concentration on big nodes. To connect different communities with randomly selected nodes does not seem a good strategy either, because there is no dynamical clustering ($Q_D \sim 0$) until the topological modularity Q_T becomes rather large. Therefore, we could speculate that communities in real-world systems shall be connected with inter-community links concentrated on the big nodes to some extent to obtain large dynamical modularity as well as better coordination among them.

V. SYNCHRONIZATION IN MODULAR CORTICAL NETWORKS

Modular organization is prominent and synchronization dynamics is of special importance for functioning in neural systems [36–40].

The critical competition regime in the synchronization of community network is of special importance from the viewpoint of information processing, where the specialized processing using the dynamical communities can coexist with the global exchange of information and integration from specialized communities. In neural systems a combination of these two ingredients, the functional segregation and integration, is believed to be crucial to underly the structural and dynamical organization for efficient and diverse functioning [41,42]. The synchronization properties of the preferential connection scheme as in the real-world cat cortical network allow quite strong global synchronization and meanwhile maintain intermediate dynamical modularity, again pointing to a meaningful balance between segregation and integration.

In order to study the relevance of this interesting observation, we study dynamics of a realistic cortical neural network of cats. The cat cortical network [43] [Fig. 6(a)] has 53 nodes, 826 weighted links, and four communities that carry out the four functions: visual (V), auditory (A), somatomotor (SM), and frontolimbic (FL). Cortical networks posses exist hub

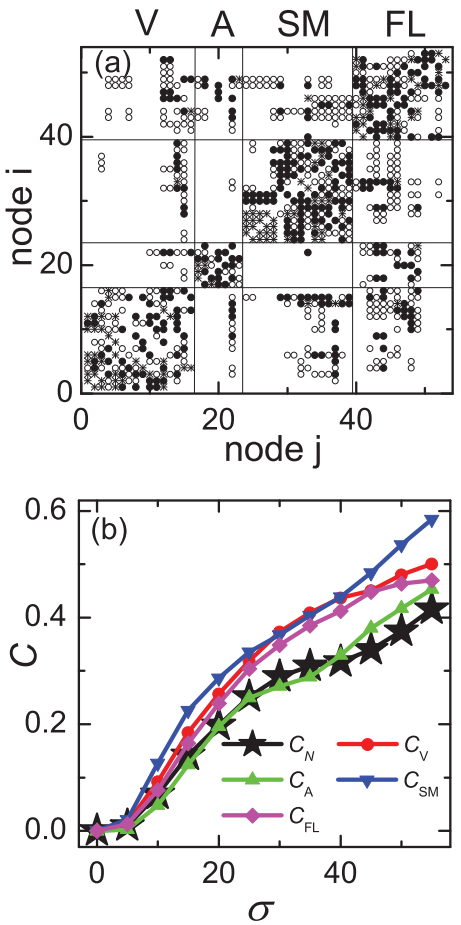

FIG. 6. (Color online) (a) The cortical network of cats. A node represents a functional region of the cortex, and a link represents the existence of fiber projection between two regions. The different symbols represent different connection weight: 1 (○ sparse), 2 (● intermediate), and 3 (∗ dense). The communities and functional subdivision V, A, SM, and FL of the network are indicated by the solid lines. (b) The change of synchronization performance of global network (C_N) and of the four communities (C_V, C_A, C_{SM}, and C_{FL}) vs the coupling strength σ. Each plot is obtained after the averaging of 10 initial states.

areas with large degree [32] and display the scale-free features [33,44]. In this network, each node represents a brain area that is composed of a huge number of interacting neurons. The rhythmic activity of such a neural ensemble can be modeled by neurophysiologically realistic neural mass oscillators [45]. The dynamical equation of coupled neural mass model is [36]

$$\begin{aligned} \ddot{v}_i^P &= Aaf\left(v_I^E - v_i^I\right) - 2a\dot{v}_i^P - a^2 v_i^P, \\ \ddot{v}_i^I &= BbC_4 f\left(C_3 v_i^P\right) - 2b\dot{v}_i^I - b^2 v_i^I, \\ \ddot{v}_i^E &= Aa\left[C_2 f\left(C_1 v_I^p\right) + p_i(t) + \frac{\sigma}{\langle S\rangle}\sum_j^N W_{ij}\, f\left(v_j^E - v_j^I\right)\right] \\ &\quad -2a\dot{v}_j^E - a^2 v_j^E, \end{aligned} \tag{4}$$

where v_i^P, v_i^I, and v_i^E are the average postsynaptic membrane potentials of pyramidal cells, excitatory interneurons, and inhibitory interneurons of the area i, respectively. A static nonlinear sigmoid function $f(v) = 2e_0/(1 + e^{r(v_0 - v)})$ converts the average membrane potential v into an average pulse density of action potentials. Here v_0 is the postsynaptic potential corresponding to a firing rate of e_0, and r is the steepness of the activation. The parameters A and B represent the average synaptic gains, and $1/a$ and $1/b$ the average dendritic-membrane time constants. C_1 and C_2, C_3, and C_4 are the average number of synaptic contacts for the excitatory and inhibitory synapses, respectively, and p_i represents afferent inputs from subcortical systems. A more detailed interpretation and the standard parameter values of this model can be found in Ref. [45]. We take the parameters as in Ref. [45] so that the model generates alpha-band periodic oscillations. As in Ref. [45], in our simulations we take the subcortical input as $p_i(t) = p_0 + \xi_I(t)$, where $\xi_I(t)$ is a Gaussian white noise with standard deviation $D = 2$. W_{ij} is the coupling strength from area j to area i. We normalize coupling strength σ by the mean intensity $\langle S\rangle$, where the connection intensity $S_i = \sum_j^N W_{ij}$ is the total input weight to node i.

In this system of noisy oscillations, we also use the correlation between nodes to measure the network synchronization performance. Figure 6(b) shows the change of C_N and C_C of the four communities with coupling strength σ. Unlike in Fig. 1(a), here we do not observe the region III where C_N decreases with σ; however, there is a regime at intermediate couplings where C_N increases slowly.

In order to see if the real system could work in the balance and critical states, we compare the synchronization performance of the real network with rewired networks having larger or smaller topological modularity. This is obtained by rewiring the intra-community links to inter-community links or rewiring the inter-community links to intra-community links

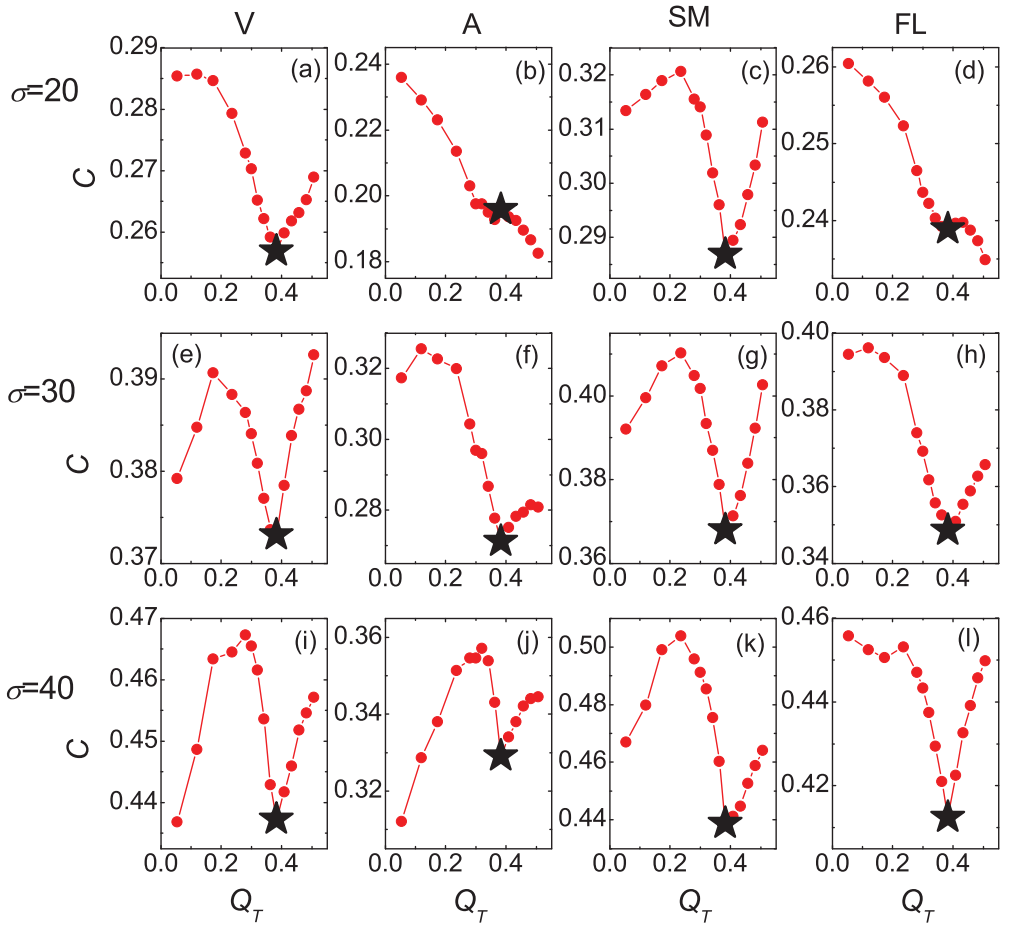

FIG. 7. (Color online) The change of C_C vs Q_T at $\sigma = 20.0$, 30.0, and 40.0. The stars present the results of the original cat cortical network. Each plot is obtained after averaging over 50 network configurations and 10 initial states of each configuration.

of the original cat cortical network. Figure 7 shows the change of C_C of the four communities with respect to Q_T (solid dot lines). Interestingly, in a broad coupling strength region, the original network (star) is just at the critical point of topological modularity where C_C is a minimum simultaneously in several or all the communities. These results confirmed our expectation that the real cortical network is organized such that it allows efficient global integration under the condition that the functional segregation is also maintained simultaneously. This finding provides a detailed mechanism for our previous observation [22] that the dynamical complexity measuring a balance between segregation and integration is optimal in cat cortical networks.

VI. DISCUSSION AND CONCLUSION

In summary, we have studied in detail the effects of inter-community links on the synchronization performance of community networks. We have revealed an interesting competition between synchronization of the global network and the individual communities. With the increasing of the number of inter-community links the global network synchronization will be enhanced, but the synchronization performance of individual community will be degraded till a critical point where the community structure is no longer prominent. Afterwards, synchronization within the community increases again as part of the global network. We also investigated the impact of various connection strategies on the global and community synchronization. We showed that connecting nodes selected randomly in different communities will ensure better global network synchronization but weak dynamical modularity. On the other hand, concentrating all the inter-community links to nodes with largest degrees may not be efficient for global integration of the whole network.

Interestingly, these discoveries in generic models are demonstrated to be relevant in a realistic cat cortical network with simulated neural population activities. Comparing the synchronization properties to rewired networks with larger or small modularity, we found that the real network is just at the critical point. Our analysis indicates that the cat cortical network is organized such that it allows both segregated performance with the communities and efficient integration of the whole network.

Our work has provided a deeper understanding how the inter-community link number and connection strategy affect the synchronization of community networks as a whole as well as individual community. These results not only present the possible reason for the real cortical network to evolve to the current community structure from the dynamical point of view but also provide useful methods to regulate the synchronization of community networks for potential applications.

ACKNOWLEDGMENTS

This work is supported by the National Natural Science Foundation of China (Grant No. 10805045), the key project of the Ministry of Education of China (Grant No. 210166), Guangxi Normal University, and Hong Kong Baptist University and the Hong Kong Research Grants Council (HKBU 202710).

[1] M. E. J. Newman, Phys. Rev. E **64**, 016131 (2001).
[2] M. Girvan and M. E. J. Newman, Proc. Natl. Acad. Sci. USA **99**, 7821 (2002).
[3] G. Palla, I. Derényi, I. Farkas, and T. Vicsek, Nature (London) **435**, 814 (2005).
[4] L. Huang, K. Park, Y.-C. Lai, L. Yang, and K. Yang, Phys. Rev. Lett. **97**, 164101 (2006).
[5] T. Zhou, M. Zhao, G. Chen, G. Yan, and B.-H. Wang, Phys. Lett. A **368**, 431 (2007).
[6] X. H. Wang, L. C. Jiao, and J. S. Wu, Chin. Phys. B **19**, 020501 (2010).
[7] K. Park, Y. C. Lai, S. Gupte, and J. W. Kim, Chaos **16**, 015105 (2006).
[8] S. G. Guan, X. G. Wang, Y.-C. Lai, and C. H. Lai, Phys. Rev. E **77**, 046211 (2008).
[9] H. J. Wang, H. B. Huang, G. X. Qi, and L. Chen, Europhys. Lett. **81**, 60005 (2008).
[10] K. H. Wang, X. C. Fu, and K. Z. Li, Chaos **19**, 023106 (2009).
[11] E. Oh, K. Rho, H. Hong, and B. Kahng, Phys. Rev. E **72**, 047101 (2005).
[12] G. Yan, Z. Q. Fu, J. Ren, and W. X. Wang, Phys. Rev. E **75**, 016108 (2007).
[13] A. Arenas, A. Díaz-Guilera, and C. J. Pérez-Vicente, Phys. Rev. Lett. **96**, 114102 (2006).
[14] S. Boccaletti, M. Ivanchenko, V. Latora, A. Pluchino, and A. Rapisarda, Phys. Rev. E **75**, 045102 (2007).
[15] E. Oh, C. Choi, B. Kahng, and D. Kim, Europhys. Lett. **83**, 68003 (2008).
[16] D. Gfeller and P. De Los Rios, Phys. Rev. Lett. **100**, 174104 (2008).
[17] X. J. Li, M. H. Li, Y. Q. Hu, Z. R. Di, and Y. Fan, Physica A **389**, 164 (2010).
[18] A. Arenas and A. Díaz-Guilera, Eur. Phys. J. Spec. Top. **143**, 19 (2007).
[19] J. Gómez-Gardeñes, Y. Moreno, and A. Arenas, Phys. Rev. Lett. **98**, 034101 (2007).
[20] M. Brede, Eur. Phys. J. B **62**, 87 (2008).
[21] E. Fuchs, A. Ayali, E. Ben-Jacob, and S. Boccaletti, Phys. Biol. **6**, 036108 (2009).
[22] M. Zhao, C. Zhou, Y. Chen, B. Hu, and B. H. Wang, Phys. Rev. E **82**, 046225 (2010).
[23] M. Brede, Europhys. Lett. **90**, 60005 (2010).
[24] D. Li, I. Leyva, J. A. Almendral, I. Sendiña-Nadal, J. M. Buldú, S. Havlin, and S. Boccaletti, Phys. Rev. Lett. **101**, 168701 (2008).
[25] L. M. Pecora and T. L. Carroll, Phys. Rev. Lett. **80**, 2109 (1998).
[26] M. Barahona and L. M. Pecora, Phys. Rev. Lett. **89**, 054101 (2002).
[27] M. E. J. Newman and M. Girvan, Phys. Rev. E **69**, 026113 (2004).

[28] M. E. J. Newman, Phys. Rev. E **70**, 056131 (2004).
[29] A. Arenas, A. Díaz-Guilera, and C. J. Pérez-Vicente, Physica D **224**, 27 (2006).
[30] P. Erdös and A. Rényi, Publ. Math. Debrecen **6**, 290 (1959).
[31] P. Erdös and A. Rényi, Magyar Tud. Akad. Mat. Kutató Int. Közl. **5**, 17 (1960).
[32] O. Sporns, C. J. Honey, and R. Kötter, PLoS ONE **2**, e1049 (2006).
[33] M. Kaiser, R. Martin, P. Andras, and M. P. Young, Euro. J. Neurousci **25**, 3185 (2007).
[34] A.-L. Barabási and R. Albert, Science **286**, 509 (1999).
[35] G. Zamora-Lopez, C. S. Zhou, and J. Kurths, Front. Neuroinfomatics **4**, Article 1 (2010).
[36] C. S. Zhou, L. Zemanova, G. Zamora-Lopez, C. C. Hilgetag, and J. Kurths, New J. Phys. **9**, 178 (2007).
[37] C. C. Hilgetag and M. Kaiser, Neuroinformatics **2**, 353 (2004).
[38] L. Zemanová, C. S. Zhou, and J. Kurths, Physica D **224**, 202 (2006).
[39] C. Zhou, L. Zemanová, G. Zamora, C. C. Hilgetag, and J. Kurths, Phys. Rev. Lett. **97**, 238103 (2006).
[40] D. Meunier, R. Lambiotte, and E. T. Bullmore, Front. Neurosci. **4**, 200 (2010).
[41] G. Tononi, O. Sporns, and G. M. Edelman, Proc. Natl. Acad. Sci. USA **91**, 5033 (1994).
[42] O. Sporns, G. Tononi, and G. M. Edelman, Cereb. Cortex **10**, 127 (2000).
[43] J. W. Scannell, G. A. P. C. Burns, C. C. Hilgetag, M. A. O'Neil, and M. P. Young, Cereb. Cortex **9**, 277 (1999).
[44] G. Zamora-Lopez, Changsong Zhou, and J. Kurths, Chaos **19**, 015117 (2009).
[45] F. Wendling, J. J. Bellanger, F. Bartolomei, and P. Chauvel, Biol. Cybern. **83**, 367 (2000).